



# Spontaneous orbital decompression in thyroid eye disease: new measurement methods and its influential factors

Aric Vaidya<sup>1</sup> · Patricia Ann L. Lee<sup>1</sup> · Yoshiyuki Kitaguchi<sup>2</sup> · Hirohiko Kakizaki<sup>1</sup> · Yasuhiro Takahashi<sup>1</sup> 

Received: 12 March 2020 / Revised: 12 May 2020 / Accepted: 19 May 2020 / Published online: 25 May 2020  
© Springer-Verlag GmbH Germany, part of Springer Nature 2020

## Abstract

**Purpose** To evaluate spontaneous decompression of the medial orbital wall and orbital floor in thyroid eye disease using new measurement methods and to analyze the influential factors.

**Methods** This retrospective study included 86 patients (172 sides). Regarding evaluation of spontaneous medial orbital decompression, an anteroposterior line was drawn between the posterior lacrimal crest and the junction between the ethmoid bone and corpus ossis sphenoidalis. The bulged and/or dented areas from that line were measured. Regarding evaluation of spontaneous orbital floor decompression, the length of the perpendicular distance from a line that was drawn between the inferior orbital rim and the orbital process of palatal bone to the tip of the superior bulge of the orbital floor was measured.

**Results** Multivariate linear regression analysis revealed that the maximum cross-sectional areas of the superior rectus/levator palpebrae superioris complex ( $P = 0.020$ ) and medial rectus muscle ( $P = 0.028$ ) were influential factors for spontaneous decompression of medial orbital wall (adjusted  $r^2 = 0.090$ ;  $P < 0.001$ ), whereas the number of cycles of steroid pulse therapy ( $P = 0.002$ ) and the maximum cross-sectional area of the inferior rectus muscle ( $P = 0.007$ ) were the ones for that of the orbital floor (adjusted  $r^2 = 0.096$ ;  $P < 0.001$ ).

**Conclusion** We believe that the identification of multiple influential factors of spontaneous decompression of the medial orbital wall and orbital floor will be helpful for better understanding and planned management of thyroid eye disease patients undergoing orbital decompression surgery.

**Keywords** Spontaneous decompression · Medial wall · Orbital floor · Thyroid eye disease · Compressive optic neuropathy

## Introduction

Spontaneous orbital decompression is expressed as a flattening (Fig. 1a) and further bowing/fracture (Fig. 1b and c) of a naturally convex-shaped medial orbital wall and orbital floor (Fig. 1d and e) [1, 2]. This is caused by any pathologically elevated intraorbital pressure without any known etiology, such as trauma, orbital surgical history, or orbital bony pathology [1, 2]. As these orbital walls are thin and vulnerable to high intraorbital pressure, expansion of the intraorbital soft tissue in patients with thyroid eye disease (TED) promotes such orbital bone remodeling [1, 3]. Spontaneous orbital

decompression reduces the intraorbital pressure at the orbital apex and subsequently lessens the risk of compressive optic neuropathy (CON) [3].

There have been several studies on spontaneous orbital decompression and its influential factors [1, 3–9]. For evaluation of spontaneous medial orbital wall decompression, all the previous reports had measured the angle between the decompressed part and the straight line through the medial orbital wall or the lateral orbital wall [1, 3, 5, 6], except the study done by Bokman et al., which measured the distance between the decompressed part and the straight line through the medial orbital wall [8]. These measurement procedures are applicable to patients with a convex or concave medial orbital wall. However, in patients with a flattened medial orbital wall, as the shape of the wall is irregular (Fig. 1a), the degree of spontaneous decompression is difficult to be evaluated by measurements of the angle and the distance. Besides, a previous study used an axial computed tomographic (CT) image through an upper orbit for measurement of the medial wall bowing [8]. Normally, the anatomy of the medial orbital wall

✉ Yasuhiro Takahashi  
yasuhiro\_tak@yahoo.co.jp

<sup>1</sup> Department of Oculoplastic, Orbital & Lacrimal Surgery, Aichi Medical University Hospital, 1-1 Yazako-Karimata, Nagakute, Aichi 480-1195, Japan

<sup>2</sup> Department of Ophthalmology, Osaka University, Suita, Osaka, Japan

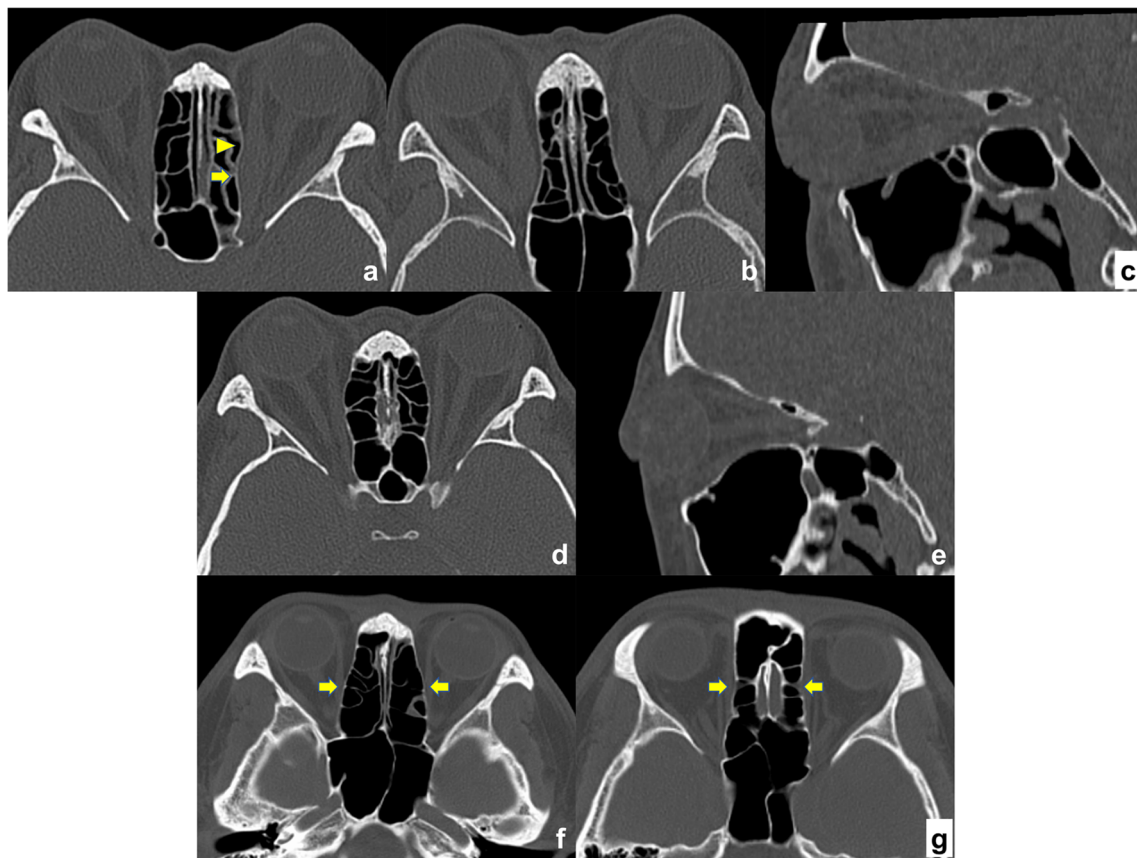


**Fig. 1** The shape of the medial orbital wall and orbital floor (a). The flattened/mixed pattern of the medial orbital wall on the left side. The irregular left medial orbital wall shows mixed convex (arrow head) and concave (arrow) parts (b). The concave pattern of the medial orbital wall on both sides (c). A sagittal computed tomographic image showing the concave pattern of the orbital floor with a negative measurement value of

the length of the superior bulge (d, e). Convex-shaped medial orbital walls on both sides (d) and orbital floor (e), (f, g). Anatomy of the medial orbital wall in a healthy individual. The medial orbital wall is bulged at the middle to lower level of the orbit (arrows) (f) but is dented at the upper level of the orbit (arrows) (g)

shows a convex shape in the middle to lower orbit (Fig. 1f), while a concave shape is usually seen in the upper orbit (Fig. 1g). This may be misleading the oculoplastic surgeons toward the false notion of spontaneous orbital decompression.

On the other hand, there is only one report on spontaneous orbital floor decompression in a large case series [3]. In this study, the angle between the medial orbital wall and the orbital floor was measured on coronal CT images; however, a convex shape and its probable changes can be better detectable on sagittal planes (Fig. 1c and e).

To counteract those defects, we present new techniques for the objective quantification of spontaneous decompression of the medial orbital wall and orbital floor, and investigate the possible influential factors of those clinical entities in TED.

## Methods

### Study design

This study was a retrospective chart review of consecutive Japanese patients with TED in whom CT was taken for

preoperative preparation of orbital decompression surgery between January 2016 and January 2019. All patients were euthyroid at the time of taking CT. Patients who had undergone orbital decompression surgery at another clinic before referral to us, those who had sustained orbital fracture previously, and those with other concomitant orbital diseases were excluded from this study. None of the patients had taken oral prednisolone before taking CT.

### Data collection

The data on age, sex, the period from the onset of TED to the time when CT was taken, the number of cycles of steroid pulse therapy that the patients had undergone until taking CT, preoperative Hertel exophthalmometric values, preoperative intraocular pressure, and the presence or absence of CON were collected from the medical charts of all the patients. The Hertel exophthalmometer was measured by 2 of the authors (HK and YT). CON was diagnosed based on optic nerve compression seen on imaging without other causes of vision loss and including at least one of the following: visual acuity of 0.5

or less, central flicker frequency of 35 Hz or less, positive relative afferent pupillary defect, central or paracentral scotoma, and papilloedema or a pale optic disc [10].

## Measurements on CT

Contiguous 1-mm axial, coronal, and quasi-sagittal (parallel to the optic nerve) CT images (Aquilion 64; Toshiba, Tokyo, Japan) were obtained using bone and soft tissue window algorithms. All measurements were performed using the digital caliper and the freehand measuring tools of the image viewing software (ShadeQuest/ViewR; Yokogawa Medical Solutions Corporation, Tokyo, Japan) by one of the authors (YT).

The degree of spontaneous decompression of the medial orbital wall and orbital floor was evaluated on the axial CT image showing the maximum cross-section area of the medial rectus muscle (MRM) and on the quasi-sagittal CT image through the optic nerve with bone window, respectively. For evaluation of spontaneous medial orbital wall decompression, the anteroposterior line was drawn between the posterior lacrimal crest and the junction between the ethmoid bone and corpus ossis sphenoidalis, and its length was measured as the medial orbital wall length (Fig. 2a and b). This junction is easily detectable because the bone thickness changes from an anterior thin bone to a posterior thick bone. If the axial CT slice passed above the level through the junction between the anterior and posterior lacrimal crests, the line was drawn from the anterior lacrimal crest. Next, the bulged and/or dented areas from the line were measured (Fig. 2a and b). The shape of the medial orbital wall was classified into 3 patterns as follows: the convex (Fig. 1d) and concave patterns (Fig. 1b) showing only bulged and hollow areas of the medial orbital wall, respectively, and the mixed pattern (Fig. 1a) presenting mixed bulged and hollow areas. Then, the number of the ethmoid septa that attached to the medial orbital wall was counted and the anteroposterior length of the medial wall of the longest ethmoid cell in the anteroposterior direction (the length of the longest cell) was measured (Fig. 2a and b). For evaluation of spontaneous orbital floor decompression, a line was drawn between the inferior orbital rim and the orbital process of the palatal bone (Fig. 2c and d). Next, the length of the perpendicular distance from that line to the tip of the superior bulge of the orbital floor (the length of the superior bulge) was measured (Fig. 2c and d). Then, on coronal CT images, the presence or absence of Haller cell was confirmed (Fig. 2e) because the septum of Haller cell supports the orbital floor [11].

The maximum cross-sectional areas of the superior rectus/levator palpebrae superioris (SR/LPS) complex, inferior rectus muscle (IRM), MRM, and superior oblique muscle (SOM) were measured on coronal CT images with soft tissue window showing the maximum cross section of them. Similarly, those of the lateral rectus muscle (LRM) and inferior oblique muscle (IOM) were measured on the axial CT image showing the

whole length of the LRM and on the quasi-sagittal CT image through the optic nerve with soft tissue window, respectively [12].

## Statistical analysis

The patient's age and measurement results were expressed as means  $\pm$  standard deviations. Patients were classified into 3 groups, based on the shape of the medial orbital wall (group 1, convex pattern; group 2, mixed pattern; group 3, concave pattern). The bulged and dented areas of the medial orbital wall were expressed as positive and negative values, respectively. In group 2, the bulged and dented areas were added. The length of the superior bulge was expressed as a positive value when the orbital floor had superiorly bulged. The patient's age, the period from the onset of TED to the time when CT was taken, the number of cycles of steroid pulse therapy, Hertel exophthalmometric values, intraocular pressure, the length of the medial orbital wall, the number of ethmoid septa, the length of the longest cell, and each extraocular muscle area were compared between the groups using one-way ANOVA and Tukey-Kramer post hoc test. The ratio of patients with or without CON was compared between the groups using the chi-square test. Variables that could influence the total sum area, such as patient age, the period from the onset of TED to the time when CT was taken, the number of cycles of steroid pulse therapy, Hertel exophthalmometric values, intraocular pressure, presence or absence of CON, the length of the medial orbital wall, the number of ethmoid septa, the length of the longest cell, and each extraocular muscle area were evaluated via univariate and multivariate linear regression analyses with stepwise variable selection. Similarly, variables that could influence the length of the superior bulge, such as patient age, the period from the onset of TED to the time when CT was taken, the number of cycles of steroid pulse therapy, Hertel exophthalmometric values, intraocular pressure, presence or absence of CON, each extraocular muscle area, and presence or absence of Haller cell were evaluated via univariate and multivariate linear regression analyses with stepwise variable selection. The presence or absence of CON and Haller cell (0 = absence, 1 = presence) was expressed using a binary system (a dummy variable) for analyses. All statistical analyses were performed using SPSS™ ver. 26 software (IBM Japan, Tokyo, Japan). A *P* value of  $< 0.05$  was considered statistically significant.

**Results** In 93 patients, CT was taken before orbital decompression surgery, but 7 patients were excluded from this study because of history of orbital decompression surgery before referral to us (5 patients), medial orbital wall fracture (1 patient), or concomitant orbital metastasis of breast cancer (1 patient). This study included 172 sides from 86 patients with

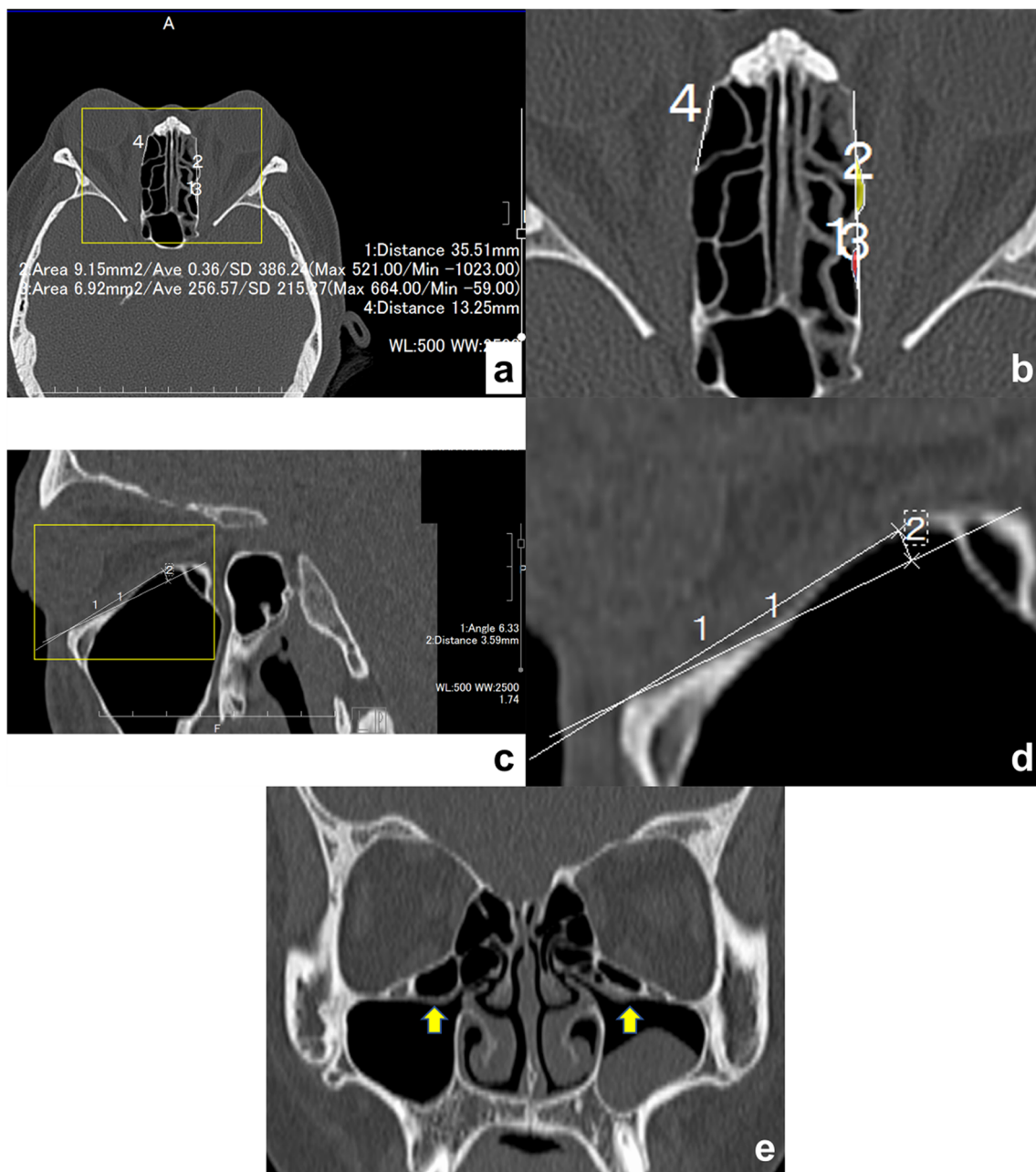


**Fig. 2** Evaluation of spontaneous medial orbital wall decompression (**a**, **b**). The image is same as Fig. 1a. On the axial computed tomographic (CT) image showing the maximum cross-section area of the medial rectus muscle, the length of the line from the posterior lacrimal crest to the junction between the ethmoid bone and corpus ossis sphenoidalis was measured as the length of the medial orbital wall (#1). The bulged (#2, yellow area on **b**) and dented (#3, red area on **b**) areas of the medial orbital wall from the line were measured. In addition, the anteroposterior length of the medial wall of the longest ethmoid cell in the anteroposterior

direction (the length of the longest cell) (#4) was measured. Panel **b** is an enlarged view of the rectangular area in **a**. Evaluation of spontaneous orbital floor decompression (**c**, **d**). On the quasi-sagittal CT image through the optic nerve, the line between the inferior orbital rim and the orbital process of the palatal bone was drawn. Then, the length of the perpendicular distance between that line and the tip of the superior bulge of the orbital floor (the length of the superior bulge) was measured (#2). Panel **d** is an enlarged view of the rectangular area in **c**. Haller cells (arrows) (**e**)

TED. Patient demographic data and measurement results are shown in Table 1.

The statistical results of the inter-group comparison are shown in Table 2. Groups 1, 2, and 3 included 112 (65.1%), 44 (25.6%), and 16 sides (9.3%), respectively. Patients in group 2 were older than those in group 1 ( $P = 0.002$ ) and

group 3 ( $P = 0.028$ ). In addition, patients in group 2 showed thicker SR/LPS complex ( $P < 0.001$ ), IRM ( $P = 0.019$ ), and MRM ( $P = 0.001$ ) than those in group 1. Similarly, patients in group 3 demonstrated thicker SR/LPS complex than those in group 1 ( $P = 0.009$ ), although the difference in the cross-sectional area of the MRM between the groups 1 and 3 did not



**Table 1** Patient data and measurement results

Number of patients/sides	
Total	86/172
Male	12/24
Female	74/148
Age (range) (years)	39.2 ± 14.5 (15 to 95)
Period from onset to time to take CT (months) (range)	48.4 ± 66.8 (1 to 408)
Cycles of steroid pulse therapy (range)	1.4 ± 2.0 (0 to 9)
Hertel exophthalmometric value (mm) (range)	20.8 ± 2.8 (12 to 28)
Intraocular pressure (mm Hg) (range)	16.6 ± 3.2 (10 to 29)
Number of patients/sides with CON	9/14
Number of sides	
Group 1 (convex shape)	112 (65.1%)
Group 2 (mixed shape)	44 (25.6%)
Group 3 (concave shape)	16 (9.3%)
Total sum area of medial orbital wall (mm <sup>2</sup> ) (range)	31.6 ± 33.5 (−91.3 to 101.5)
Length of medial orbital wall (mm) (range)	36.9 ± 3.0 (28.3 to 45.8)
Number of ethmoid septa (range)	4.4 ± 1.2 (1 to 7)
Length of the longest cell (mm) (range)	12.2 ± 3.2 (6.0 to 27.5)
Length of superior bulge (mm) (range)	2.8 ± 1.1 (−1.2 to 6.1)
Number of sides with Haller cell	17
Maximum cross-sectional areas of extraocular muscles (mm <sup>2</sup> ) (range)	
SR/LPS complex	46.1 ± 17.6 (20.5 to 136.2)
IRM	45.7 ± 13.6 (20.1 to 117.7)
LRM	120.5 ± 33.1 (56.4 to 246.3)
MRM	40.6 ± 14.6 (19.6 to 111.0)
SOM	18.0 ± 5.9 (5.3 to 42.3)
IOM	27.2 ± 11.8 (7.7 to 62.3)

CT, computed tomography; CON, compressive optic neuropathy; SR/LPS, superior rectus/levator palpebrae superioris; IRM, inferior rectus muscle; LRM, lateral rectus muscle; MRM, medial rectus muscle; SOM, superior oblique muscle; IOM, inferior oblique muscle

reach statistical significance ( $P = 0.067$ ). The ratio of patients with or without CON was different between the groups ( $P < 0.001$ ).

Statistical results of univariate and following multivariate linear regression analyses are shown in Table 3. Univariate analysis showed that the total sum of areas of the medial orbital wall was correlated with the length of the medial orbital wall ( $P = 0.029$ ), the number of ethmoid septa ( $P = 0.035$ ), and the maximum cross-sectional areas of the SR/LPS complex ( $P < 0.001$ ), IRM ( $P = 0.005$ ), and MRM ( $P < 0.001$ ). Multivariate stepwise analyses revealed that the maximum cross-sectional areas of the SR/LPS complex ( $P = 0.020$ ) and MRM ( $P = 0.028$ ) were influential factors for spontaneous decompression of the medial orbital wall (adjusted  $r^2 = 0.090$ ;  $P < 0.001$ ).

Univariate analysis showed that the length of the superior bulge of the orbital floor was correlated with the patient age ( $P = 0.001$ ), the number of cycles of steroid pulse therapy ( $P = 0.001$ ), and the maximum cross-sectional areas of the IRM ( $P = 0.002$ ), MRM ( $P = 0.017$ ), and SOM ( $P = 0.033$ ). Multivariate stepwise analyses revealed that the number of

cycles of steroid pulse therapy ( $P = 0.001$ ), Hertel exophthalmometric value ( $P = 0.043$ ), and the maximum cross-sectional area of the IRM ( $P = 0.003$ ) were influential factors for spontaneous decompression of the orbital floor (adjusted  $r^2 = 0.112$ ;  $P < 0.001$ ). However, as there was collinearity between the Hertel exophthalmometric value and the maximum cross-sectional area of the IRM, the Hertel exophthalmometric value was deleted from this analysis because this value was not correlated with the length of the superior bulge of the orbital floor confirmed by univariate analysis. Multivariate stepwise re-analysis revealed that the number of cycles of steroid pulse therapy ( $P = 0.002$ ) and the maximum cross-sectional area of the IRM ( $P = 0.007$ ) were influential factors for spontaneous decompression of the orbital floor (adjusted  $r^2 = 0.096$ ;  $P < 0.001$ ).

Among 60 orbits in groups 2 and 3, the anteroposterior position of the thickest part of an enlarged MRM corresponded to that of the largest ethmoid cell in 34 sides (56.7%).

Only a single side of one patient demonstrated a negative value of the length of the superior bulge (0.6%) (Fig. 1c).

**Table 2** Statistical results of inter-group comparison

	One-way ANOVA	Groups 1 vs. 2	Groups 1 vs. 3	Groups 2 vs. 3
Age	0.002	0.002	0.839	0.028
Period from onset to time to take CT	0.912	-	-	-
Cycles of steroid pulse therapy	0.148	-	-	-
Hertel exophthalmometric value	0.346	-	-	-
Intraocular pressure	0.738	-	-	-
Length of medial orbital wall	0.096	-	-	-
Number of ethmoid septa	0.487	-	-	-
Length of the longest cell	0.474	-	-	-
Maximum cross-sectional areas		-	-	-
SR/LPS complex	< 0.001	< 0.001	0.009	0.935
IRM	0.022	0.019	0.558	0.749
LRM	0.946	-	-	-
MRM	< 0.001	0.001	0.067	0.969
SOM	0.437	-	-	-
IOM	0.239	-	-	-

CT, computed tomography; SR/LPS, superior rectus/levator palpebrae superioris; IRM, inferior rectus muscle; LRM, lateral rectus muscle; MRM, medial rectus muscle; SOM, superior oblique muscle; IOM, inferior oblique muscle

## Discussion

This study investigated spontaneous decompression of the medial orbital wall and the orbital floor in TED using new measurement methods and analyzed its influential factors.

Our study demonstrated that maximum cross-sectional areas of the MRM and IRM were influential factors for spontaneous decompression of each corresponding orbital wall, respectively. This implies that the direct pressure from enlarged extraocular muscles onto the orbital walls, rather than diffusely elevated intraorbital pressure, more strongly pushes the walls [3]. These results of our study were partially corresponding to those of the previous studies regarding the influence of the size of the MRM in spontaneous medial orbital wall decompression [1, 7, 8].

Further multivariate stepwise analyses revealed that the maximum cross-sectional area of the SR/LPS complex was also an influential factor for spontaneous medial orbital wall decompression. None of the previous studies had investigated the significance of the dimension of the SR/LPS complex. As enlargement of the SR/LPS complex and MRM is frequently accompanied by that of the other extraocular muscles in Japanese patients [13], the enlargement of the muscle complex may indicate a severe TED with high intraorbital pressure. This may result in a high incidence of spontaneous medial orbital wall decompression in such cases.

Several previous studies argued about the relationship between spontaneous orbital decompression and CON. Bokman et al. found that radiological identification of medial wall bowing was associated with clinical measures of disease severity, including CON [8]. Chan et al. also demonstrated that the

orbital angle was a predictive factor for CON [6]. On the contrary, Kang et al., Tan et al., and Weis et al. reported no relationship between changes in the shape of the medial orbital wall and CON [1, 3, 5]. Our study agrees with the results of these previous 3 reports [1, 3, 5]. Although enlargement of the extraocular muscles causes CON, this also induces spontaneous orbital decompression and consequent decreased risk of CON; hence, resulting in no relationship between spontaneous orbital decompression and CON in this study.

We found out that patients in group 2 were older than those in group 1. In addition, patients in group 2 showed thicker SR/LPS complex, IRM, and MRM than those in group 1. As elderly patients demonstrate the weakening of the bone density due to osteoporosis and higher severity of TED with greater changes in the enlarged extraocular muscles [14], they may be more vulnerable to have a mixed pattern regarding the shape of the medial orbital wall.

Previous reports hypothesized that the patients with a fewer ethmoid air cell septa and a larger lamina papyracea area per septum are more likely to develop isolated medial wall fractures than inferior wall fractures when similar extrinsic forces acted on the periocular region [15, 16]. However, Kang et al. showed that the development of spontaneous medial orbital wall decompression was not associated with the structure of ethmoid bone or sinus [1]. Our present study also showed that the number of ethmoid septa and the length of the longest ethmoid cell did not affect spontaneous medial orbital wall decompression. In addition, although approximately half of the orbits showed correspondence between the anteroposterior location of the thickest part of the MRM and the largest ethmoid cell, the others did not. This implies that the enlarged

**Table 3** Statistical results of univariate and following multivariate linear regression analysis with stepwise variable selection

	Univariate		Multivariate stepwise	
	<i>P</i> value	Crude coefficient (95% CI)	<i>P</i> value	Crude coefficient (95% CI)
Total sum areas of medial orbital wall				
Age	0.299	−0.184 (−0.533 to 0.164)	-	-
Period from onset to time to take CT	0.535	0.024 (−0.052 to 0.100)	-	-
Cycles of steroid pulse therapy	0.138	−1.909 (−4.440 to 0.622)	-	-
Hertel exophthalmometric value	0.277	−0.999 (−2.806 to 0.808)	-	-
Intraocular pressure	0.492	−0.550 (−2.127 to 1.027)	-	-
Presence or absence of CON	0.371	−8.391 (−26.850 to 10.068)	-	-
Length of medial orbital wall	0.029	1.859 (0.192 to 3.526)	-	-
Number of ethmoid septa	0.035	4.433 (0.306 to 8.560)	-	-
Length of the longest cell	0.488	−0.550 (−2.115 to 1.014)	-	-
Maximum cross-sectional areas				
SR/LPS complex	<0.001	−0.520 (−0.797 to −0.244)	0.020	−0.365 (−0.672 to −0.058)
IRM	0.005	−0.529 (−0.892 to −0.165)	-	-
LRM	0.689	0.010 (−0.040 to 0.061)	-	-
MRM	<0.001	−0.616 (−0.952 to −0.280)	0.028	−0.416 (−0.787 to −0.044)
SOM	0.621	−0.215 (−1.072 to 0.642)	-	-
IOM	0.082	−0.377 (−0.802 to 0.049)	-	-
Length of superior bulge of orbital floor				
Age	0.001	−0.018 (−0.030 to −0.007)	-	-
Period from onset to time to take CT	0.841	0 (−0.002 to 0.003)	-	-
Cycles of steroid pulse therapy	0.001	−0.143 (−0.225 to −0.062)	0.002	−0.129 (−0.210 to −0.049)
Hertel exophthalmometric value	0.345	0.029 (−0.031 to 0.088)	-	-
Intraocular pressure	0.465	−0.019 (−0.071 to 0.033)	-	-
Presence or absence of CON	0.186	−0.408 (−1.015 to 0.198)	-	-
Presence or absence of Haller cell	0.813	0.067 (−0.492 to 0.626)	-	-
Maximum cross-sectional areas				
SR/LPS complex	0.104	−0.008 (−0.017 to 0.002)	-	-
IRM	0.002	−0.019 (−0.031 to −0.007)	0.007	−0.016 (−0.028 to −0.005)
LRM	0.361	−0.001 (−0.002 to 0.001)	-	-
MRM	0.017	−0.014 (−0.025 to −0.003)	-	-
SOM	0.033	−0.030 (−0.058 to −0.002)	-	-
IOM	0.432	−0.006 (−0.020 to 0.008)	-	-

CT, computed tomography; CI, confidence interval; CON, compressive optic neuropathy; SR/LPS, superior rectus/levator palpebrae superioris; IRM, inferior rectus muscle; LRM, lateral rectus muscle; MRM, medial rectus muscle; SOM, superior oblique muscle; IOM, inferior oblique muscle

MRM can cause spontaneous medial orbital wall decompression, irrespective of the location of the weakest point in the medial orbital wall and the degree of wall strength.

The number of cycles of steroid pulse therapy was found to be an influential factor for spontaneous orbital floor decompression. Systemic steroids may increase bone resorption, reduce osteoblastic activity, and result in osteoporosis in adults [3, 17, 18]. Therefore, in TED, due to the effects of treatment with intravenous or oral steroids, a tendency toward microarchitectural weakening in the orbital bones may be a permissive factor that allows for the occurrence of remodeling of the bone under the stress of an increased intraorbital soft

tissue volume and pressure [3]. This explains our finding of the number of cycles of steroid pulse therapy as the influential factor for spontaneous orbital floor decompression.

The period between the onset of TED and the time when CT was taken did not influence spontaneous orbital decompression. The cumulative time a patient remains hyperthyroid is also a risk factor for major osteoporotic fractures, as there is an imbalance between bone resorption and formation that might result in decreased bone mineral density [3, 19–21]. In addition, long-term pressure onto the orbital walls is suspected to cause greater denting of the walls. As all the patients in our study were euthyroid at the time of surgery,

the above result tends to imply that the duration of the hyperthyroid state of those patients might have been short.

Bokman et al. found that 12% of their patients demonstrated medial wall bowing [8]. Similarly, a study by Kang et al. estimated the incidence of spontaneous medial orbital wall decompression to be 5.51% [1]. In contrast, our present study showed that 34.9% of the orbits (groups 2 and 3) showed spontaneous medial orbital wall decompression, which is higher than that of the previous studies [1, 8]. This disparity may be due to the difference in techniques of evaluation of spontaneous medial orbital wall decompression. Moreover, we included only those patients who were planned for orbital decompression. Therefore, we can infer that the severity of TED might have been higher in our patient group, possibly resulting in a higher percentage of patients with spontaneous medial orbital wall decompression.

On the contrary, only a single side of one patient demonstrated that of the orbital floor with a negative value of the length of the superior bulge (0.6%). The medial orbital wall, being the thinnest wall of the orbit, maybe more pliable to bony remodeling secondary to raised intraorbital pressures than the orbital floor [3]: another possible reason being that the IRM runs near the junction between the medial orbital wall and the orbital floor, where the inferomedial orbital strut attaches. As this is thicker than the ethmoid septa, the orbital floor can better resist the direct pressure from the enlarged IRM.

There are a few limitations to this study. First, as this study had a retrospective design, its validity should be evaluated in a future prospective study. Second, the orbital anatomy shows a racial difference [22]. Moreover, Japanese patients usually show milder TED than other races [23]. Therefore, the results of our study performed in Japanese people may not be applicable to other races.

In conclusion, we evaluated spontaneous decompression of the medial orbital wall and orbital floor in TED using new measurement methods, and multiple influential factors were identified in this study. We believe our results will be helpful for better understanding and planned management of TED patients undergoing orbital decompression surgery.

**Authors' contributions** All authors qualify for authorship based on contributions to the conception and design (YT), acquisition of data (YT), statistical analysis (YK and YT), literature search (AV and YT), and interpretation of data (all authors). All authors contributed to drafting the article and revising it critically for important intellectual content and final approval of the version to be published. No one contributed to the work who did not meet our authorship criteria.

**Data availability** All data are included in this report.

### Compliance with ethical standards

**Conflict of interest** The authors declare that they have no conflict of interest.

**Ethics approval** This study was approved by the Institutional Review Board (IRB) of our institution (Aichi Medical University Hospital, approval No. 2019-175) and followed the tenets of the 1964 Declaration of Helsinki.

**Consent to participate** The IRB granted a waiver of informed consent for this study on the basis of the ethical guidelines for medical and health research involving human subjects established by the Japanese Ministry of Education, Culture, Sports, Science, and Technology and the Ministry of Health, Labour, and Welfare. The waiver was granted because the study was a retrospective review and not an interventional study and because it was difficult to obtain consent from patients who had been treated several years prior to this study. Nevertheless, at the request of the IRB, an outline of the study was published on the website of our institution and this was made available for public viewing. This public posting also gave patients an opportunity to decline participation, although no refusal was made known to us. Personal identifiers were removed from the records prior to data analysis.

### References

- Kang EM, Yoon JS (2015) Clinical and radiological characteristics of Graves' orbitopathy patients showing spontaneous decompression. *J Craniomaxillofac Surg* 43:48–52
- Kahaly GJ (2001) Imaging in thyroid-associated orbitopathy. *Eur J Endocrinol* 145:107–118
- Tan NYQ, Leong YY, Lang SS, Htoon ZM, Young SM, Sunder G (2017) Radiologic parameters of orbital bone remodeling in thyroid eye disease. *Invest Ophthalmol Vis Sci* 58:2527–2533
- Bhermi GS, Gauba V, Brittain P (2006) Spontaneous bony orbital auto-decompression in thyroid ophthalmopathy. *Orbit* 25:123–125
- Weis E, Heran MK, Jhamb A, Chan AK, Chiu JP, Hurley MC, Rootman J (2012) Quantitative computed tomographic predictors of compressive optic neuropathy in patients with thyroid orbitopathy: a volumetric analysis. *Ophthalmology* 119:2174–2178
- Chan LL, Tan HE, Fook-Chong S, Teo TH, Lim LH, Seah LL (2009) Graves ophthalmopathy: the bony orbit in optic neuropathy, its apical angular capacity, and impact on prediction of risk. *Am J Neuroradiol* 30:597–602
- Detorakis ET (2014) Spontaneous medial orbital decompression associated with medial wall remodeling in Graves' orbitopathy. *Ophthalmic Plast Reconstr Surg* 30:79–80
- Bokman CL, Ugradar S, Rootman DB (2018) Measurement of medial wall bowing and clinical associations in thyroid eye disease. *Ophthalmic Plast Reconstr Surg* 34:557–559
- Kashkouli MB, Pakdel F (2010) Spontaneous orbital floor fracture in thyroid eye disease. *Ophthalmic Plast Reconstr Surg* 26:301–302
- Blandford AD, Zhang D, Chundury RV, Perry JD (2017) Dysthyroid optic neuropathy: update on pathogenesis, diagnosis, and management. *Expert Rev Ophthalmol* 12:111–121
- Takahashi Y, Nakano T, Miyazaki H, Kakizaki H (2016) An anatomical study of the orbital floor in relation to the infraorbital groove: implications of predisposition to orbital floor fracture site. *Graefes Arch Clin Exp Ophthalmol* 254:2049–2055
- Sabundayo MS, Kakizaki H, Takahashi Y (2018) Normative measurements of inferior oblique muscle thickness in Japanese by magnetic resonance imaging using a new technique. *Graefes Arch Clin Exp Ophthalmol* 256:839–844
- Murakami Y, Kanamoto T, Tuboi T, Maeda T, Inoue Y (2001) Evaluation of extraocular muscle enlargement in dysthyroid ophthalmopathy. *Jpn J Ophthalmol* 45:622–627
- Valencia MRP, Miyazaki H, Kakizaki H, Takahashi Y (2020) Thickness of retro- and sub-orbicularis oculi fat in thyroid eye



- disease: comparison with controls and its influential factors. *Ophthalmic Plast Reconstr Surg*. <https://doi.org/10.1097/IOP.0000000000001597>
15. Song WK, Lew H, Yoon JS, Oh MJ, Lee SY (2009) Role of medial orbital wall morphologic properties in orbital blow-out fractures. *Invest Ophthalmol Vis Sci* 50:495–499
  16. Takahashi Y, Nakakura S, Sabundayo MS, Kitaguchi Y, Miyazaki H, Mito H, Kakizaki H (2018) Differences in common orbital blow-out fracture sites by age. *Plast Reconstr Surg* 141:893e–901e
  17. Haugeberg G, Griffiths B, Sokoll KB, Emery P (2004) Bone loss in patients treated with pulses of methylprednisolone is not negligible: a short term prospective observational study. *Ann Rheum Dis* 63:940–944
  18. LoCascio V, Bonucci E, Imbimbo B, Ballanti P, Adami S, Milani S, Tartarotti D, DellaRocca C (1990) Bone loss in response to long-term glucocorticoid therapy. *Bone Miner* 8:39–51
  19. Abrahamsen B, Jørgensen HL, Laulund AS, Nybo M, Bauer DC, Brix TH, Hegedüs L (2015) The excess risk of major osteoporotic fractures in hypothyroidism is driven by cumulative hyperthyroid as opposed to hypothyroid time: an observational register-based time-resolved cohort analysis. *J Bone Miner Res* 30:898–905
  20. Vestergaard P, Rejnmark L, Mosekilde L (2005) Influence of hyper- and hypothyroidism, and the effects of treatment with anti-thyroid drugs and levothyroxine on fracture risk. *Calcif Tissue Int* 77:139–144
  21. Vestergaard P, Mosekilde L (2003) Hyperthyroidism, bone mineral, and fracture risk—a meta-analysis. *Thyroid* 13:585–593
  22. Ana-Magadia MG, Valencia MRP, Naito M, Nakano T, Miyazaki H, Kakizaki H, Takahashi Y (2020) Location of the myoneural junction of the inferior oblique muscle: an anatomic study. *Ann Anat* 227:151429
  23. Kakutani S, Ito M, Kakizaki H, Takahashi Y (in press) Orbital decompression for exorbitism and exophthalmos in a patient with thyroid eye disease. *J Craniofac Surg* in press

**Publisher's note** Springer Nature remains neutral with regard to jurisdictional claims in published maps and institutional affiliations.